Geophysical Prospecting EAGE EUROPEAN ASSOCIATION OF GEOSCIENTISTS & ENGINEERS

Geophysical Prospecting, 2009, **57**, 811–821 doi: 10.1111/j.1365-2478.2008.00773.x

Post-stack velocity analysis in the dip-angle domain using diffractions

Moshe Reshef[1,2]* and Evgeny Landa[3]

[1]*Department of Geophysics, Tel-Aviv University, Ramat Aviv, Tel-Aviv 69978, Israel,* [2]*Landmark Graphics Corporation, 1805 Shea Center Drive, Suite 400, Highlands Ranch, CO 80129, USA, and* [3]*Applied Geophysical Research Group (OPERA), IFR, rue Jules Ferry, 64000 Pau, France*

Received June 2008, revision accepted October 2008

ABSTRACT

Interval velocity analysis in complex geological areas is often considered as an unresolved problem. A novel approach to improve the velocity analysis process is to perform the analysis in a non-conventional domain and to use seismic events that are usually ignored during standard data processing and imaging. In this study, a method to analyse diffraction data for migration velocity analysis in the time- or depth-domain is presented. The method is based on the clear distinction between diffractions and reflections in the post-migration dip-angle domain. The attractive possibility to perform the analysis, using only stacked data as an input, is demonstrated on synthetic and real data examples.

INTRODUCTION

Diffracted waves contain valuable information about small-size objects such as faults, pinchouts, karsts, fractures, etc. (Landa, Shtivelman and Gelchinsky 1987; Kanasevich and Phadke 1988; Liu, Crampin and Hudson 1997; Landa and Keydar 1998; Bansal and Imhof 2005). Diffraction analysis is a challenging problem due to the fact that the energy retained by these events is typically one or two orders of magnitude weaker than the one retained by the reflections. This is the main reason why several authors claimed that diffractions should be separated from reflections before the analysis or imaging (Harlan, Claerbout and Rocca 1984; Khaidukov, Landa and Moser 2004; Moser and Howard 2008). Correct identification and use of diffraction events is important also for velocity estimation and can be carried out in the prestack (Sava, Biondi and Etgen 2005) as well as in the post-stack domain (Fomel, Landa and Taner 2007).

The post-migration dip-angle domain has gained some attention lately and was shown to be of great importance to the quality of depth imaging in complex geological areas (Audebert *et al.* 2002; Reshef and Rueger 2008). In this study, we propose to use the dip-angle domain for the development of methods to extract and analyse diffraction data. In particular we suggest using migrated diffractions for velocity analysis, in both time- and depth-domains.

In the following we first describe the dip-angle domain data decomposition after migration and show how diffraction and reflection events behave in this domain. The ability to use single offset to generate the dip-angle common-image gathers is also demonstrated. We then present, using synthetic and real data examples, the influence of velocity errors on the appearance of the migrated diffractions and conclude with a few remarks on the possibility to separate diffractions from reflections after migration.

DIFFRACTIONS IN THE DIP-ANGLE DOMAIN

In order to use diffractions for velocity analysis, a domain in which migrated diffractions will show high sensitivity to velocity variations, needs to be chosen for the analysis. We chose to use here the dip-angle common-image gathers. The main idea can be briefly described as follows. Using conventional scattering-angle or offset gathers for interval velocity analysis has shortcomings in the presence of structural complexity. The structural dip information in such cases can become crucial. This information is readily available during prestack depth migration and can be used for construction of common-image

*E-mail: moshe@luna.tau.ac.il

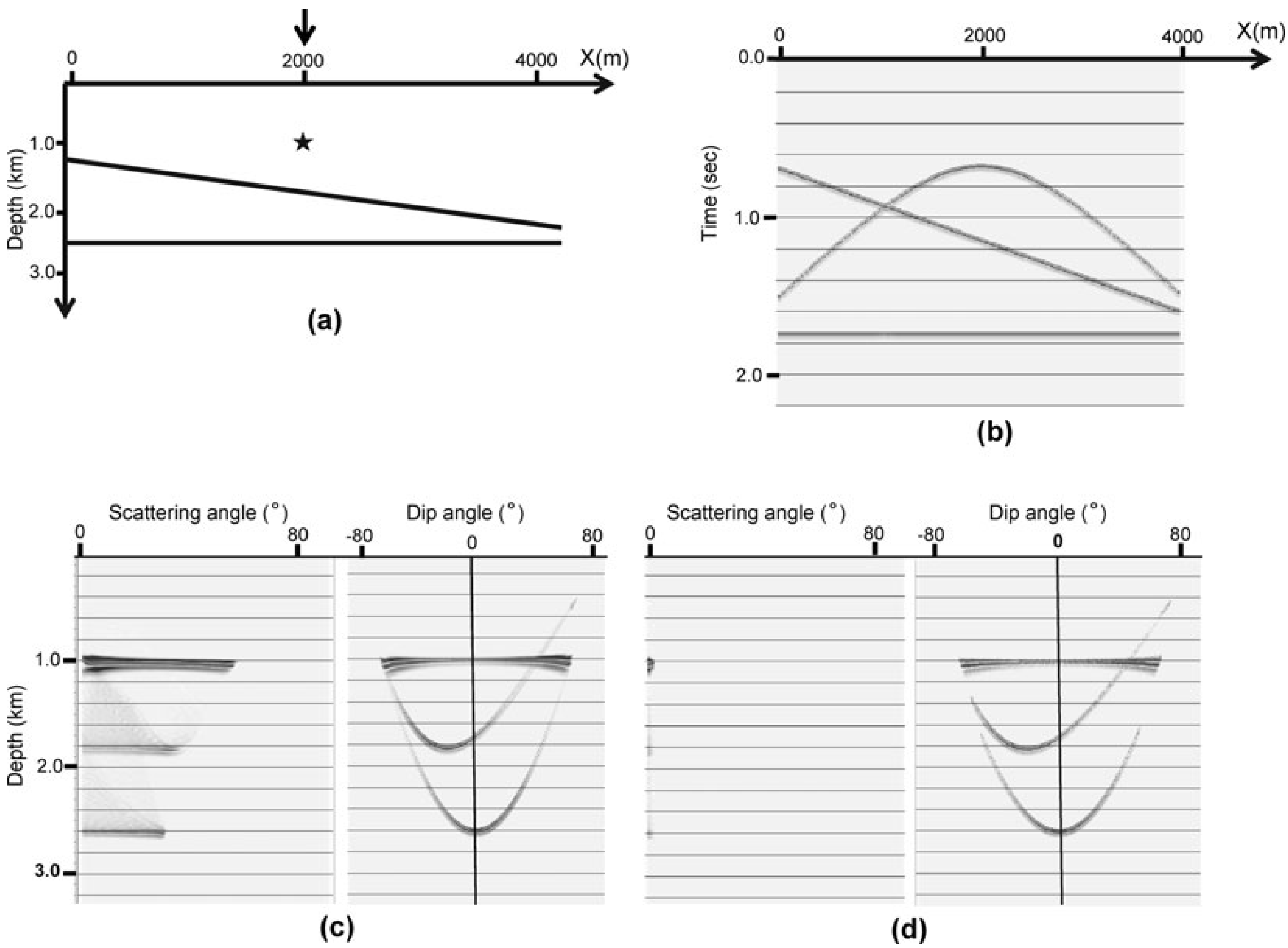

Figure 1 Diffractions and reflections in the migrated common-image gather domain. a) Synthetic model, b) zero-offset section, c) scattering-angle common-image gather (left) and dip-angle common-image gather (right) after migrating the entire dataset and d) scattering-angle common-image gather (left) and dip-angle common-image gather (right) after migrating only the zero-offset traces.

gathers. The procedure for generating these common-image gathers is described by Audebert *et al.* (2002) and Reshef and Rueger (2008). To view the unique appearance of diffracted events in these common-image gathers, let us follow the simple example presented in Fig. 1. A two-dimensional constant velocity physical model is shown in Fig. 1(a). It consists in a single diffractor (marked by the star in the figure), a dipping layer and a flat layer. 160 shots with split-spread configuration and maximum offset of 3000 m were generated over this model. Figure 1(b) presents the zero-offset section calculated for the model. A single common-image gather (see location marked by the arrow in Fig. 1a) derived from a Kirchhoff-based angle prestack depth migration (PSDM), using the correct velocity, is shown in Fig. 1(c). On the left is the conventional scattering-angle common-image gather and on the right is the dip-angle common-image gather. The flat events on the scattering-angle common-image gather clearly indicate that the migration velocity was correct. However, by examining such a scattering-angle common-image gather, there is no way to tell if a particular event is dipping or not and whether it is a reflection or diffraction. Although the stack of each common-image gather will produce exactly the same trace, the dip-angle common-image gather is quite different. In this domain, after migration with the correct velocity, reflections appear as concave-shaped events while diffractions are flat. In addition, information on the dip of the reflector can be extracted from the horizontal position of the event's minimum. We repeated the PSDM but instead of using the entire prestack data, only the zero-offset traces were input. In other words, we applied PSDM to a stack section. Figure 1(d) shows the resulted common-image gathers. The scattering-angle common-image gather (left) is useless in this case, since only one trace in

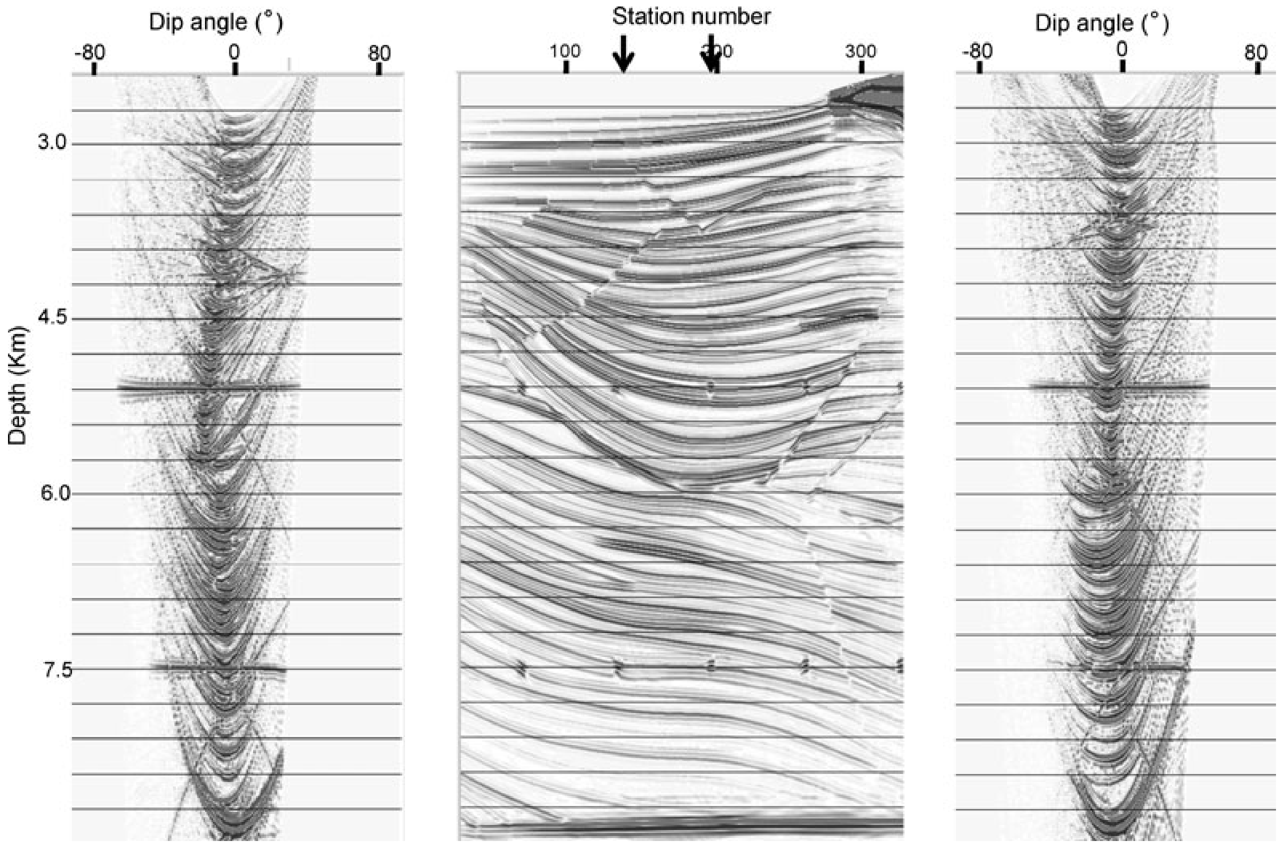

Figure 2 Final PSDM image (centre) with two dip-angle common-image gathers (left and right). The location of the common-image gathers is marked by the arrows above the depth section.

it contains migrated data. On the other hand the dip-angle common-image gathers (right) is almost identical to the one obtained by performing the migration using the entire input data. There is a significant difference in the amplitudes of the events but kinematically they are the same. A similar result would have been obtained if a different common-offset gather was used as input.

A more complicated example is presented in Fig. 2. The section in the centre is a portion of a depth image obtained after applying PSDM with the correct velocity to the entire Sigsbee synthetic dataset. Two dip-angle common-image gathers are shown on the left and on the right of the depth section. Each common-image gather is located above two diffraction points (see arrows above the central image). This example clearly shows how the flat appearance of the migrated diffractors (at a depth of 5.2 and 7.5 km) is distinguishable from the concave shape of the numerous reflections. From a kinematic point of view, the common-image gathers shown here could have been generated with a minimal amount of input traces. In Fig 3, we compare one of the common-image gathers after using only 3 offsets per input gather (Fig. 3a) and all 200 offsets per input gather (Fig. 3b). Although there are visible amplitude differences between the images, the clear dissimilarity between diffractors and reflectors is maintained in both images.

When the velocity used for the migration is the correct one, a migrated diffractor will be horizontal only at the dip-angle common-image gather located right above it. Migrated diffractions will also contribute to common-image gathers that are not located above the horizontal position of the diffractor. A visual examination of several neighbouring common-image gathers can be used to identify the diffractor's horizontal position. In Fig. 4, a set of dip-angle gathers, which were used to construct the central depth section shown in Fig. 2, are presented. The two arrows point to the lateral position of the diffractors (stations 130 and 195). We note that even on the common-image gathers not above the diffractors, the migrated diffractions (elongated dipping events with a dip direction related to their position relative to lateral position of the diffractor) can be easily differentiated from the

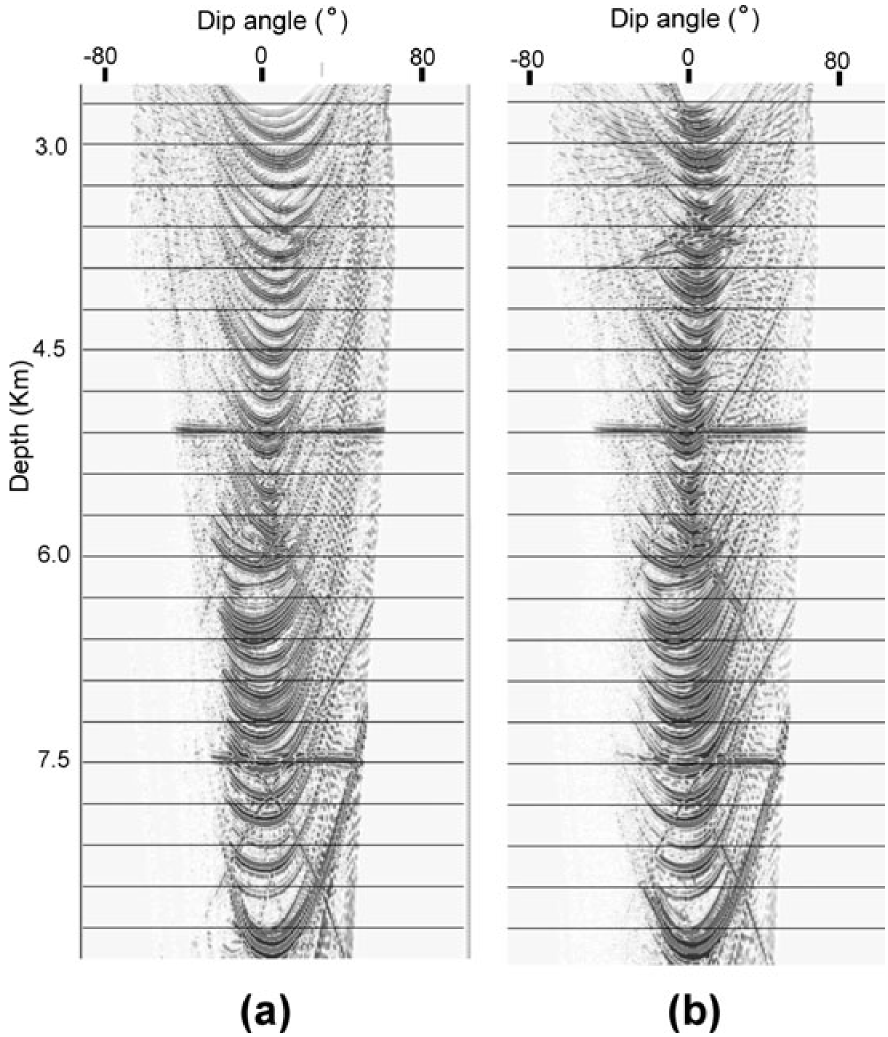

Figure 3 Comparison of two dip-angle common-image gathers obtained after PSDM using 3 offsets from each input gather (a) and 200 offsets from each input gather (b).

concave reflectors. This example demonstrates that if the velocity function is known, the location of a diffractor can be determined by identifying flat events on the dip-angle common-image gathers.

VELOCITY ANALYSIS USING MIGRATED DIFFRACTIONS

After PSDM, reflections in the dip-angle domain will always have a concave shape, regardless of the migration velocity used (Reshef 2007). It means that there is no practical way to use the reflections in this domain for velocity analysis. The effect of velocity errors on diffractions is completely different in this domain, as demonstrated by Fig. 5. The figure presents a dip-angle common-image gather after applying PSDM to the zero-offset data with a wrong velocity, too low on the left and too high on the right. The two strong diffractors in this common-image gather are marked by a dashed arrow (upper diffractor) and a solid arrow (lower diffractor). Note that while the reflections are shifted up and down (with respect to the low/high velocity) and maintain the same concave shape, the diffractions show the familiar 'smiling' and 'frowning' look. Unlike the asymmetric shape of the concave reflections, which is related to their dip (Audebert *et al.* 2002), the asymmetry of the diffractions is due to the lateral velocity variations and the location of the common-image gather with respect to the diffractor(s). It can be claimed that in this post migration domain, continuous events with convex shape are most likely diffractions migrated with a too high velocity. We can therefore suggest that for a velocity scan in this domain, one should

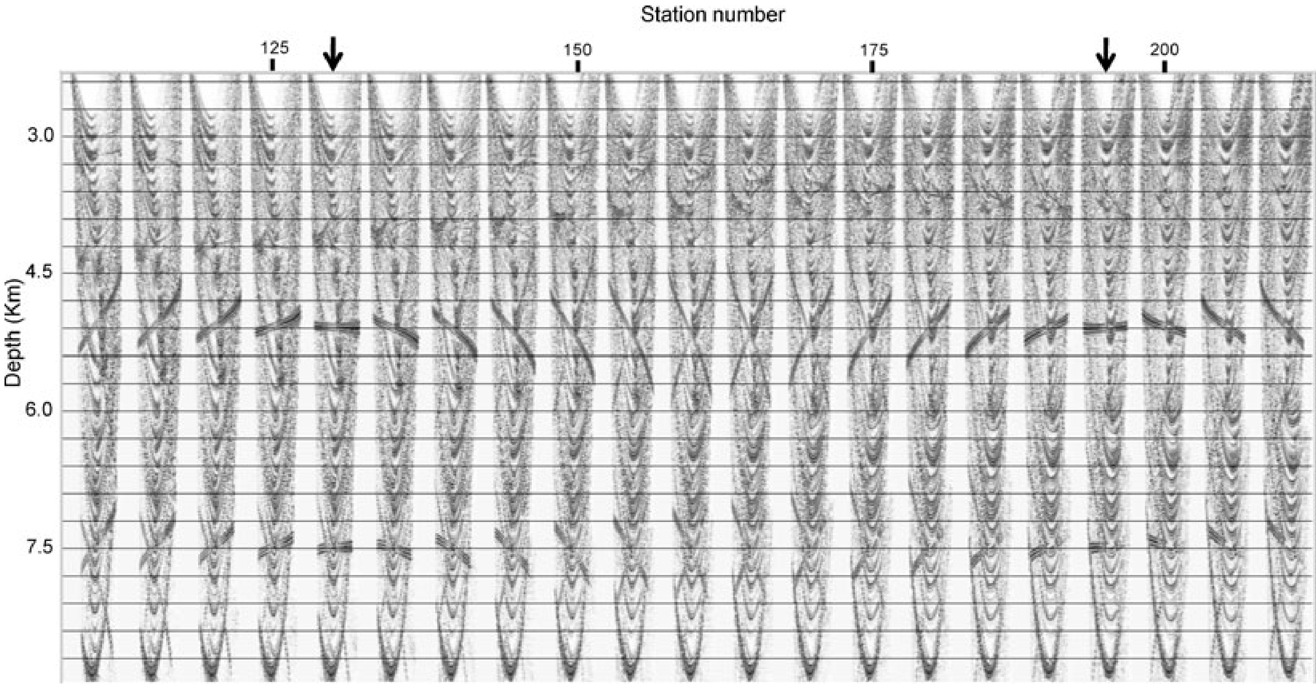

Figure 4 A set of dip-angle common-image gathers over the depth section presented in the centre of Fig. 2. The common-image gathers above the horizontal position of the diffractors (stations 130 and 195) are marked by the arrows.

start from high to low velocity until the required flatness is obtained.

The sensitivity of the diffractions to velocity errors can be used for velocity analysis. The process is demonstrated in Fig 6. Using the ability to generate dip-angle gathers from a single offset (see Fig. 1d), a prestack time migration was applied to a portion of a marine stack shown in Fig. 6(a). The single offset input (zero-offset in this case) was migrated into a set of dip-angle common-image gathers. One of the common-image gathers, located right above a diapir (see arrow on the top of Fig. 6a), is shown after application of the PSTM (Fig. 6b) with four different rms velocities, increasing by 10% increment from left to right (V4 > V3 > V2 > V1).

The examination of the migrated diffraction at 0.7 sec indicates that the second velocity (marked by V2 in the figure) is the optimal one and produces the flattest event. As in the depth-domain, the diffraction shows the classical effect of using wrong migration velocity.

PRACTICAL ISSUES

In many situations, there may be an interface in the subsurface that is rugged and therefore becomes a source of closely positioned diffractors, like for example the top of a salt body. Figure 7(a) presents a portion of a stack section calculated over an elongated salt body that is part of a larger synthetic model (Brandsberg-Dahl and Billette 2005). The data shown in Fig. 7(a) (zero-offset) were used as input to four PSDM runs. In each run a different velocity gradient was tried for the sequence between the water bottom and the top of salt. In Fig. 7(b), a comparison between the resulted common-image gathers is presented. The location of the common-image gather is marked by the vertical arrow above the input stack shown in Fig. 7(a) and the scanned gradient increases from right to left (V4 > V3 > V2 > V1). Although not as clear as in the example presented by Fig. 6, we can still follow the diffraction event that is best flattened by V2 (around 2.75 km/sec).

The flatness of the migrated diffraction can be achieved only with the correct velocity and only at a surface location right above the diffractor (see Fig. 4). The velocity scan procedure cannot be applied to a single common-image gather without the knowledge of the horizontal position of the diffractor. We therefore apply the scan to a set of common-image gathers and compare them in a way presented by Fig. 8. The figure displays the result of 3 different PSTM runs (too low velocity on top, true velocity in the middle and too high velocity at the bottom) applied to a zero-offset real dataset. The optimal velocity and the horizontal location of the diffractor are simultaneously determined (marked by the dark frame in Fig. 8).

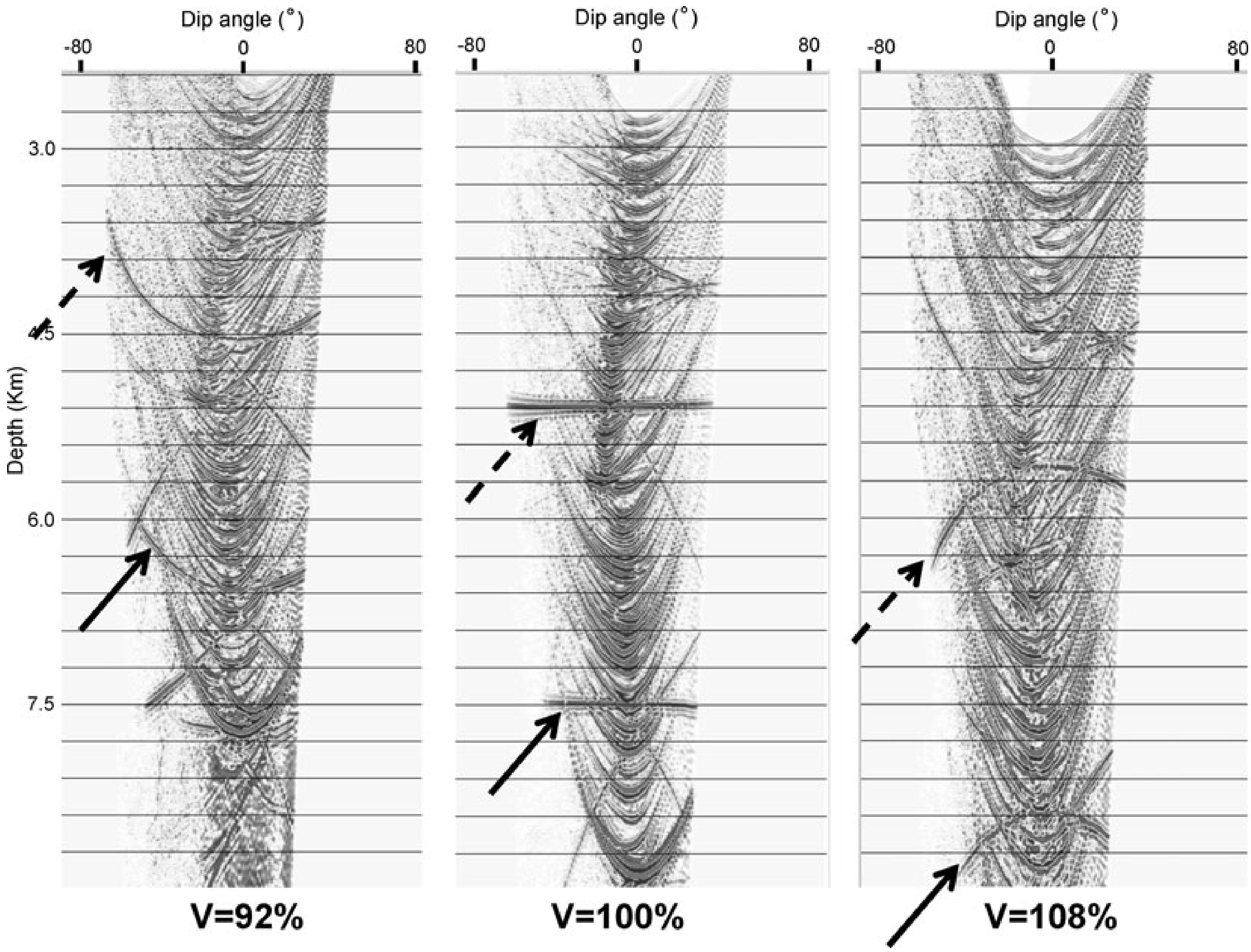

Figure 5 The effect of velocity errors. Dip angle common-image gather after migration with the correct (centre), low (left) and high (right) velocity. The two diffractors are marked by the dashed and solid arrows.

The most problematic aspect of analysing diffractions is related to their weak amplitude, compared to the reflections. The problem is demonstrated by Fig. 9 where two common-image gathers, positioned at different locations over a 2D marine line, are used for velocity analysis. In this example, the analysis is performed in the time-domain, using a stacked section as input. In Fig. 9(a), the diffractor at the time mark of about 2.1 sec is very clear and can be easily scanned for optimal flatness (appears to be the output after using V4). Selecting the optimal velocity at the second location (Fig. 9b) is not so trivial. The strong migrated reflections (appearing as concave-shaped events on the dip-angle gather) obscure the relatively weak diffraction at the time mark of about 2.5 sec. Using additional input traces (offsets) for strengthening the migrated diffractors will not help, since the amplitude of the reflections will also be enhanced. If the diffractions in this example could be separated from the reflections, then the quality and accuracy of the analysis and the diffractors' positioning would have been significantly enhanced.

To demonstrate this idea, a stack section generated after reflections was eliminated from the data (Fomel *et al.* 2007) and was taken as input for PSTM. The input data is shown at the bottom of Fig. 10. Note, that although the conventional stack does not optimally sum diffraction events, a large amount of diffraction energy is preserved in the stacked section. In principle, several procedures such as the multifocusing method (Landa *et al.* 1999) can be considered for optimally stacking diffraction events. The migration velocity was the final rms velocity and a set of dip-angle common-image gathers is displayed above the section. Note that there are no

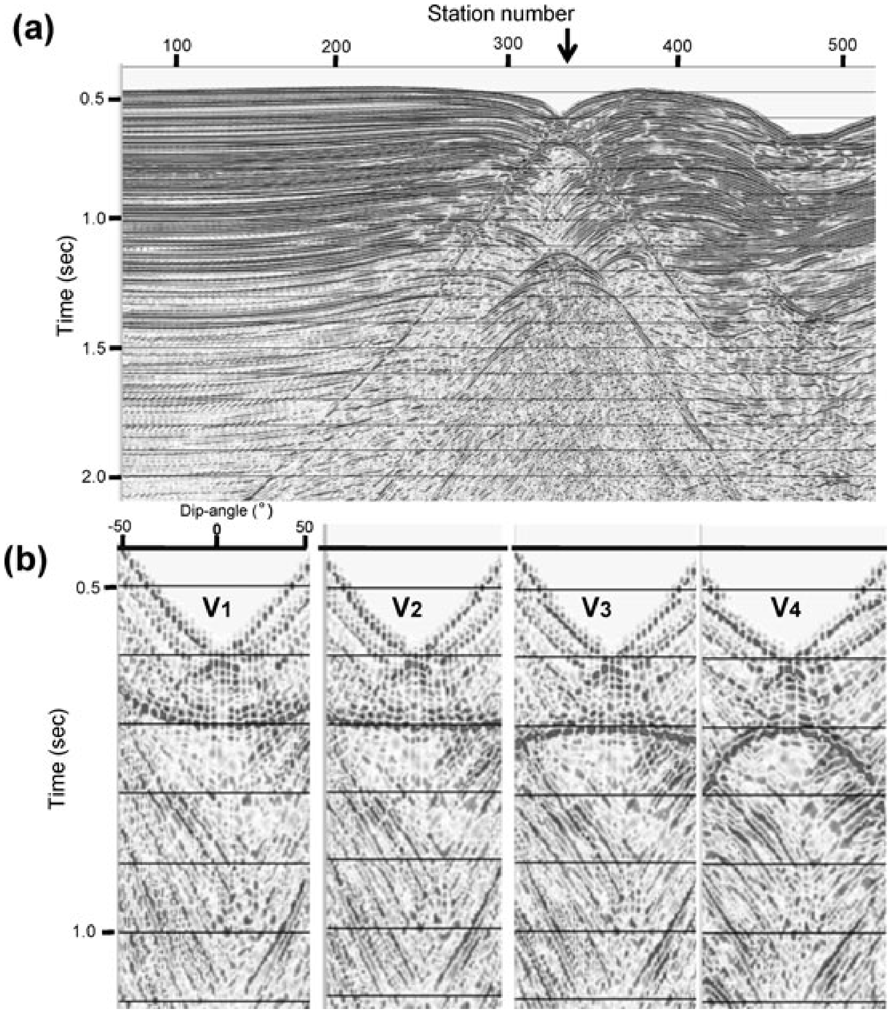

Figure 6 Post-stack diffraction velocity scan in the time-domain. a) Zero-offset section above a large diaper, used as input to the migration. b) Rms velocity scan – dip-angle common-image gather after PSTM with four velocities. The location of the analysed common-image gather is marked by the solid arrow.

concave-shaped events on the common-image gathers, indicating that the reflections' elimination was effective. The location of the few diffractors is marked by the arrows on common-image gathers 98, 101 and 113. In each of these marked locations, the migrated diffractor can be followed to both sides in which the deviation from flatness is clear. The separation of the diffracted data from the reflections results in migrated gathers with improved signal-to-noise ratio. Consequently, detailed velocity analysis and diffractor positioning can be performed even with short aperture diffractions.

Although we presented here only 2D examples, diffraction events are essentially 3D phenomena and the proposed method is valid for the 3D case as well. In 3D media, reflection surfaces beside edges may include the vertices, where several diffracting edges can intersect (tips). In this case the total diffraction wavefields contain two types of scattered events: edge-waves and tip-waves. Although the dynamic behaviour of these events is different (Klem-Musatov 1994), their kinematic part can be computed by simple ray-based algorithms.

CONCLUSIONS

There are two major advantages for migrating the prestack data into dip-angle common-image gathers. First, the appearance of the data in this domain is the same whether the input data is multi or single offset. Second, diffractions look significantly different from reflections in the common-image gathers and unlike reflections, are affected by velocity errors in the

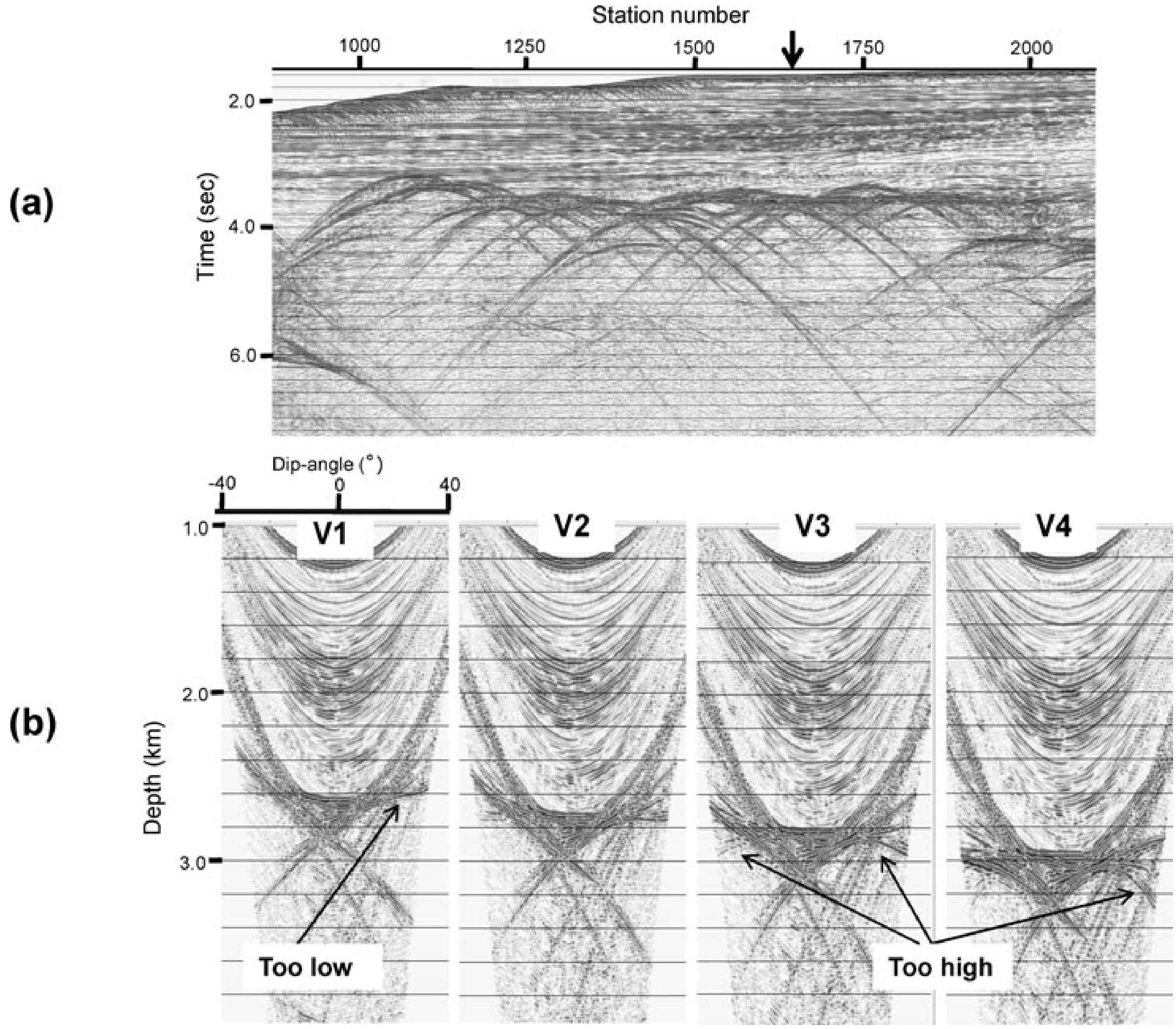

Figure 7 Interval velocity gradient scan. a) Zero-offset data above a rugged top of salt, used as input to the migration. b) Dip-angle common-image gather after PSDM with four different gradients.

conventional manner. These two characteristics can be used to apply efficient migration velocity analysis, using diffraction events. The analysis can be applied in the time- or depth- domain, using only a single-offset (zero-offset for example) as input. After the final velocity has been determined, the precise location of the diffractors can be defined by analysing the dip-angle common-image gathers. The attractive ability to perform velocity analysis using post-stack data only, offers the possibility to incorporate velocity analysis and/or velocity quality control during an interpretation session.

The distinct difference between reflections and diffractions in the migrated dip-angle domain suggest this domain as a preferable one for separating these two wavefields. The separation can be used to eliminate the migrated reflections from the common-image gathers and will improve the identification and analysis of the relatively weak diffractions. When the correct velocity is used for the migration, diffraction imaging can be performed by stacking the dip-angle common-image gathers, after application of a simple spatial filter that maintains flat events.

ACKNOWLEDGEMENTS

The authors would like to thank Reda Baina for inspiring discussions. The authors thank Total for supporting this research. OPERA is a private organization funded by Total and affiliated with Pau University.

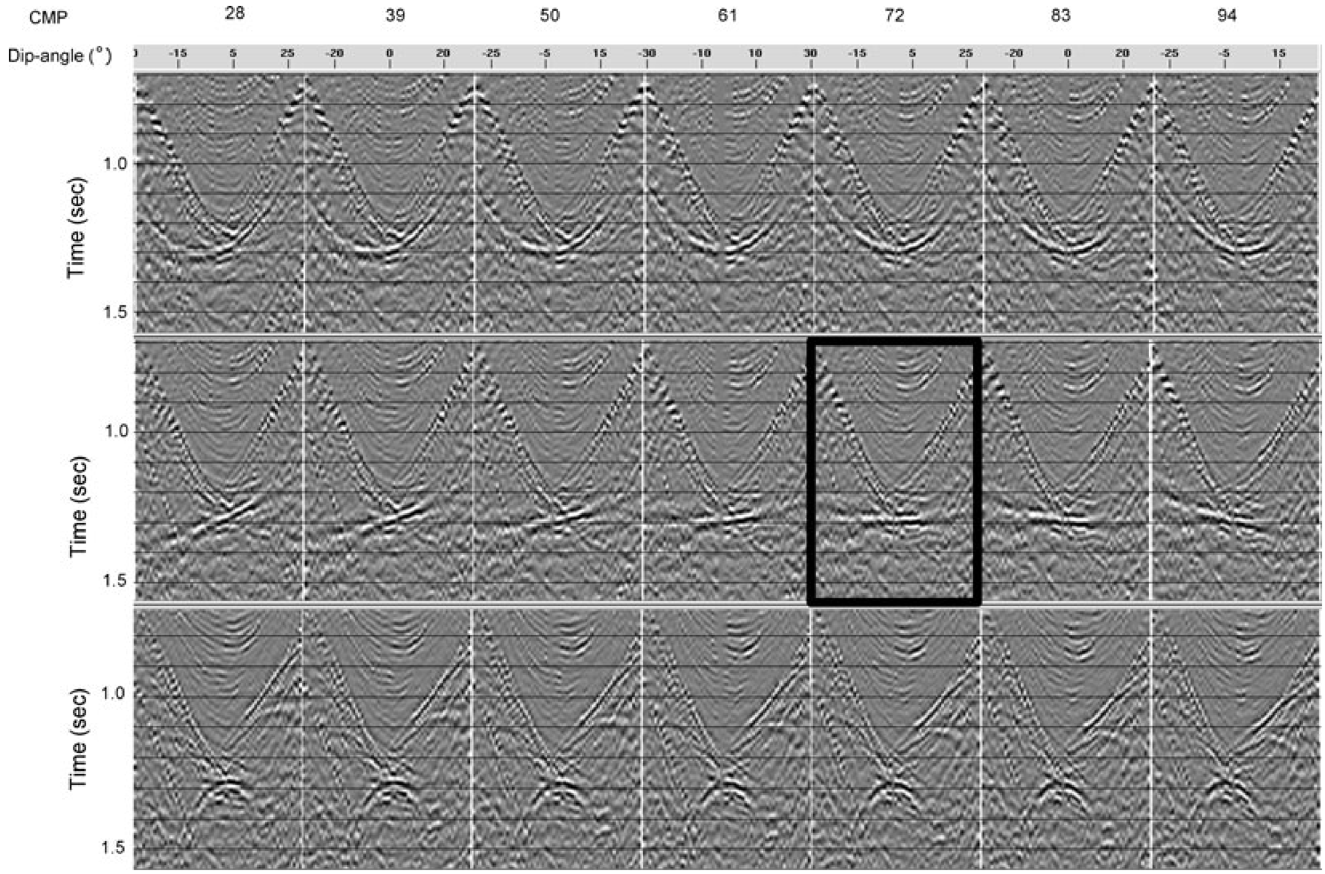

Figure 8 Simultaneous search of velocity and horizontal diffraction position. A set of dip-angle common-image gathers is shown after PSTM with too low velocity (top), too high velocity (bottom) and correct velocity (centre). The horizontal position of the analysed diffractor, at 1.3 sec is marked by the black frame (CMP 72).

REFERENCES

Audebert F., Froidevaux P., Rakotoarisoa H. and Svay-Lucas J. 2002. Insights into migration in the angle domain. 72nd SEG meeting, Salt Lake City, Utah, USA, Expanded Abstracts.

Bansal R. and Imhof M. 2005. Diffraction enhancement in prestack seismic data. *Geophysics* **70**, V73–V79.

Brandsberg-Dahl S. and Billette F.J. 2005. The 2004 BP velocity benchmark. 67th EAGE meeting, Madrid, Spain, Expanded Abstracts, B035.

Fomel S., Landa E. and Taner T. 2007. Poststack velocity analysis by separation and imaging of seismic diffractions. *Geophysics* **72**, U89–U94.

Harlan W., Claerbaut J. and Rocca F. 1984. Signal to noise separation and velocity estimation. *Geophysics* **49**, 1869–1880.

Kanasewich E. and Phadke S. 1988. Imaging discontinuities on seismic sections. *Geophysics* **53**, 334–345.

Khaidukov V., Landa E. and Moser T.J. 2004. Diffraction imaging by focusing-defocusing: an outlook on seismic super resolution. *Geophysics* **69**, 1478–1490.

Klem-Musatov K. 1994. *Theory of Seismic Diffractions*. SEG

Landa E., Gurevich B., Keydar S. and Trachtman P. 1999. Application of multifocusing method for subsurface imaging. *Applied Geophysics* **42**, 283–300.

Landa E. and Keydar S. 1998. Seismic monitoring of diffraction images for detection of local heterogeneities. *Geophysics* **63**, 1093–1100.

Landa E., Shtivelman V. and Gelchinsky B. 1987. A method for detection of diffracted waves on common-offset sections. *Geophysical Prospecting* **35**, 359–374. doi:10.1111/j.1365-2478.1987.tb00823.x

Liu E, Crampin S. and Hudson J. 1997. Diffraction of seismic waves by cracks with application to hydraulic fracturing. *Geophysics* **62**, 253–265.

Moser T.J. and Howard C.B. 2008. Diffraction imaging in depth. *Geophysical Prospecting* **56**, 627–642. doi:10.1111/j.1365-2478.2007.00718.x

Reshef M. 2007. Velocity analysis in the dip-angle domain. 69th EAGE meeting, London, UK, Expanded Abstracts.

Reshef M. and Rueger A. 2008. Influence of structural dip angles on interval velocity analysis. *Geophysics* **73**, U13–U18.

Sava P., Biondi B. and Etgen J. 2005. Wave-equation migration velocity analysis by focusing diffractions and reflections. *Geophysics* **70**, U19–U27.

(a)

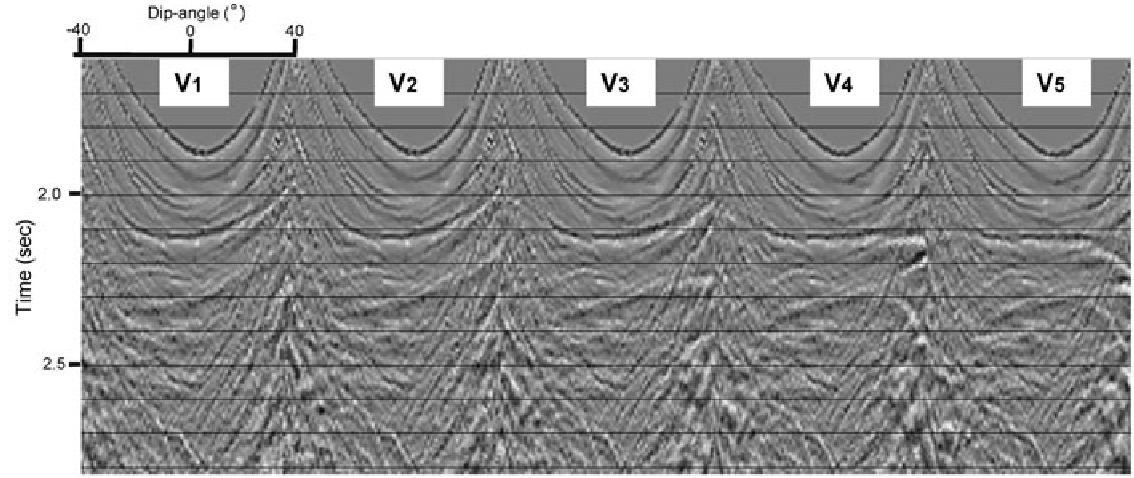

(b)

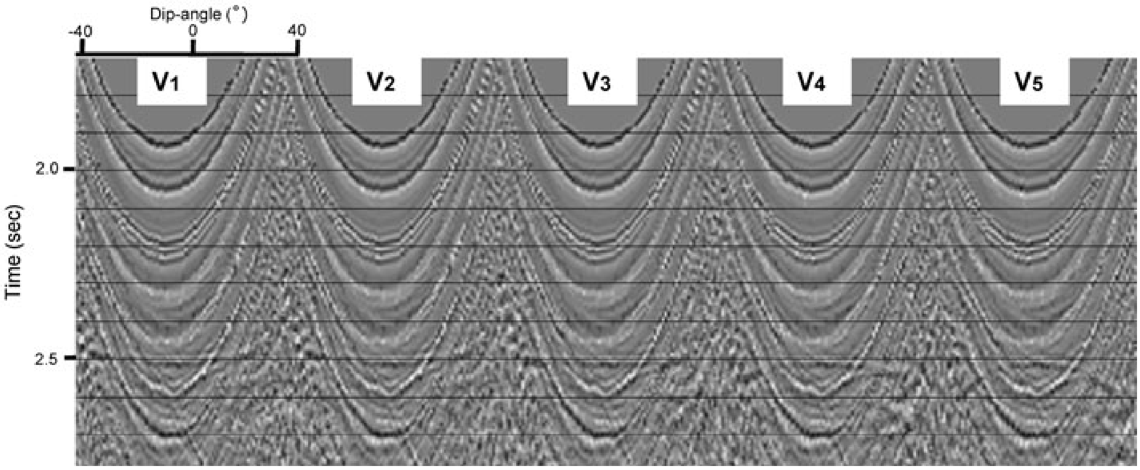

Figure 9 Rms velocity scan at a common-image gather location with weak (a) and strong (b) reflections.

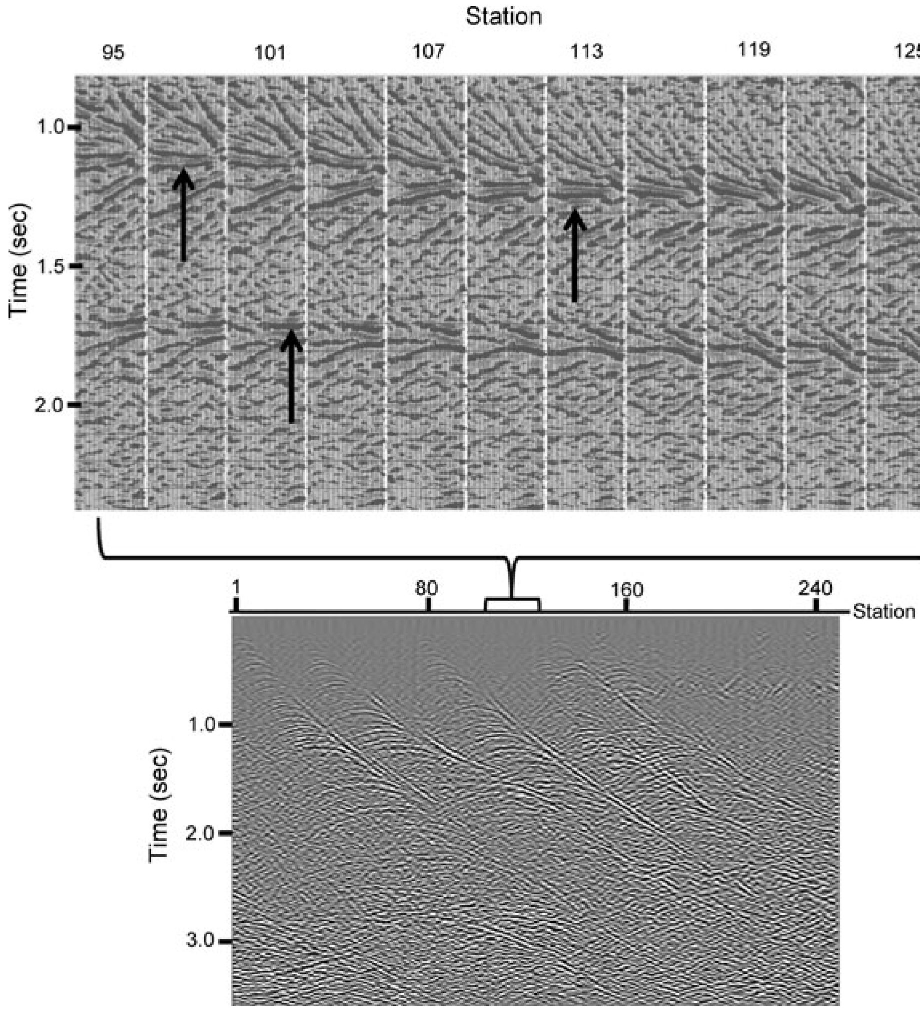

Figure 10 Diffractor positioning. Zero-offset stack, after elimination of reflection energy, used as input for PSTM (bottom image) and a set of resulting common-image gathers (top image). The flat appearance of a few diffractors is marked by the solid arrows.